INTERNATIONAL JOURNAL OF ELECTRONICS
https://doi.org/10.1080/00207217.2021.1969446

Taylor & Francis
Taylor & Francis Group

Extended bilinear transform and multirate technique based approach for analog-to-digital transform

Om Prakash Goswami[a], Dharmendra K. Upadhyay[b] and Tarun K. Rawat[b]

[a]Division of Electronics and Communication Engineering, Faculty of Technology, University of Delhi, New Delhi, India; [b]Department of Electronics and Communication Engineering, Netaji Subhas University of Technology, New Delhi, India

ABSTRACT

In this paper, a new transformation polynomial for *s*-to-*z* plane is presented. This third-order transformation is derived by optimising the coefficients of the logarithmic series followed by utilising the multirate technique to extend its bandwidth. In terms of magnitude and phase response, the proposed transform correlates well with the ideal and shows mean absolute magnitude error and mean absolute phase error as -40 dB and -132.04 dB, respectively. The proposed transform is compared with the existing operators to demonstrate its performance. In addition, an example is also conferred, which establishes the viability of the transform in terms of the overall frequency response, when applied for analog-to-digital transformation.

ARTICLE HISTORY
Received 24 Nov 2020
Accepted 20 Jun 2021

KEYWORDS
Digital filters; extended bilinear transforms; optimised operator; *s*-to-*z* transform; signal processing

1. Introduction

Nowadays, in digital filter designing, infinite impulse response (IIR) filters exhibit a broad spectrum of usage and advantages over the finite impulse response (FIR) filters. They provide the same magnitude response as the corresponding FIR filters with the lower order. Hence, the IIR filters deliver a response with less computational complexity for a similar filter roll-off as FIR. Therefore, researchers have always shown a keen enthusiasm for designing more advanced IIR filters than the existing ones. Though they have phase nonlinearity and stability issues, yet they have been resolved to some extent over recent years by utilising various techniques (Al-Alaoui, 2011a; Kim et al., 2019; Stosovic et al., 2019; Tsai & Chou, 2006; Xu et al., 2010).

There are two conventional techniques by which the IIR filters can be designed. The first technique involves the direct design in the digital domain, including the least-squares, order reduction, and pole-zero placement methods. The second technique emulates the analog prototype filter design in the digital domain by using an expropriating transformation polynomial. In the recent literature, several analog-to-digital transforms have been proposed to substitute the analog domain transfer function $H(s)$ with its equivalent transfer function $H(z)$ in the digital domain (Rawat, 2014). Transforms like bilinear and step invariant are conventionally being used so far in the filter design. The

CONTACT Om Prakash Goswami om9837@gmail.com Division of Electronics and Communication Engineering, Faculty of Technology, University of Delhi, New Delhi, 110078, India

step invariant (no hold) technique preserves the time domain specification at the sampling instants but results in aliasing. Therefore, it is unacceptable for high-pass and band-stop filters (Deng, 2016). The bilinear transform provides a piecewise linear mapping between analog and digital domain but results in the warping effect due to the non-linear relationship between analog and digital frequencies. The pre-warping has been utilised to overcome these non-linearities, but it fixes the non-linearities at the critical frequencies, not in the full Nyquist band. Therefore, it motivates designers to rethink the advanced techniques to provide the spectrum transformation without pre-warping (Dyer & Dyer, 2000; Getu, 2020).

In the recent literature, Al-Alaoui's first-, second-, third-order differentiators, Ngo's third-order differentiator, and the differentiators proposed by Schneider et al., Hsu et al., Gupta et al., and Upadhyay, have been used as *s*-to-*z* transforms (Aggarwal et al., 2017; Al-Alaoui, 2007, 2011a; Goswami et al., 2020; Gupta et al., 2010; Ngo, 2006; Pei & Hsu, 2008; Schneider et al., 1994; Upadhyay, 2012; Upadhyay & Singh, 2011).

Besides the techniques mentioned above, various optimisation algorithms have been used to design digital differentiators. These are often applied as a transformation operator to transform the *s*-plane into the *z*-plane. Some of them are based on nature-inspired algorithms like genetic algorithms (GA), particle swarm optimisation (PSO), and other modified algorithms like simulated annealing (SA), Fletcher and Powell optimisation, GGSA, etc (Aggarwal et al., 2015; Al-Alaoui & Baydoun, 2013; Gupta et al., 2014). Above mentioned techniques are intently focused on matching either the magnitude response or the phase response of *s*-plane in the digital domain. However, for the perfect *s*-to-*z* transformation, the matching of both magnitude and phase response are equally crucial for the overall frequency response of the transformed filter (Mishra et al., 2019).

In this paper, a new third-order transformation polynomial for the analog-to-digital domain is proposed. It is obtained by optimising two variables, namely α_1 and α_2, considered in the logarithmic series expansion. Then, the bandwidth of the proposed transform is extended by utilising the concept of the multirate technique. Hence, the proposed operator matches the magnitude response with the identical phase and provides a mean absolute magnitude error (MAME) as -40 dB up to the complete Nyquist interval. Consequently, the proposed operator outperforms all the existing operators in terms of MAME and mean absolute phase error (MAPE).

The rest of the paper is organised as follows: Section II deals with a brief description of the fundamental need of the perfect *s*-to-*z* transform in digital filter designing. Section-III describes the extensions of the bilinear transform with their performances. Section-IV outlines the proposed transform with their corresponding design equations and optimisation. Section-V illustrates the viability of the proposed design by showing the comparison with the extended bilinear transforms. Section-VI depicts the extension of the bandwidth for the proposed transform. Section-VII shows the comparison of the proposed transform with the existing *s*-to-*z* transforms. Section-VIII manifests the proposed design's credibility by applying it in an example, and section-IX concludes the paper.

2. Motivation

In IIR digital filter design, the fundamental requirement of the transformation from the *s*-plane to the *z*-plane can be fulfilled by choosing a suitable transformation operator. In transformation, an ideal Laplace operator '*s*' of analog domain for $-\infty \leq \Omega \leq \infty$ is defined as the one that has frequency response $H(j\omega) = j\omega$ for $-\pi \leq \omega \leq \pi$ in digital domain. The corresponding magnitude response is $|H(j\omega)| = \omega$, where ω is the angular frequency in radians, and the phase response remains as $\pi/2$ (Getu, 2020; Rawat, 2014). The analog (*s*-plane) to digital (*z*-plane) transformation operator should be chosen such that it provides linearity in the magnitude and phase as $\pi/2$. The relationship between the *s*-plane and the *z*-plane is given by

$$z = e^{sT} \tag{1}$$

where T is the sampling period in seconds. If $s = \sigma + j\Omega$ and $z = re^{j\omega}$, then equivalent relation can be formulated (Rawat, 2014)

$$re^{j\omega} = e^{\sigma T} e^{j\Omega T}$$

Considering the stability concernment of the analog and digital domain, the value of $\sigma = 0$ and $r = 1$ is taken. It implies $\omega = \Omega$ for $T = 1$. Therefore,

$$s = j\omega = f(z)|_{z=e^{j\omega}} = \omega e^{j(\pi/2)} \tag{2}$$

Ideally, the magnitude of $f(z)$ should vary linearly with ω and phase should remain as $\pi/2$ for the whole Nyquist range. However, all the proposed operators in the literature do not attain the transformation without any variation in matching magnitude or phase strictly. Consequently, if $\delta\omega$ and $\delta\phi$ are the variations in the linearity of magnitude and the ideal phase respectively, then $f(z)$ can be written as

$$f(z) = (\omega \pm \delta\omega)e^{j(\pi/2 \pm \delta\phi)} \tag{3}$$

Therefore, all the existing operators belong to either of the two classifications. First, the operators with the prefect phase, but showing variation in the magnitude response due to $\delta\omega \neq 0$. Second, the operators offering linearity in the magnitude response but do not provide the perfect phase due to $\delta\phi \neq 0$. However, for perfectly matching frequency response of the digital transformed filter, the *s*-to-*z* operator is necessary to have $\delta\omega = 0$ and $\delta\phi = 0$.

Case-I (when $\delta\phi \rightarrow 0$ and $\delta\omega \neq 0$)

If there is no variation in the transformation operator's phase response and it remains $\pi/2$ for the full Nyquist range. It directs us to the bilinear transform, which provides the perfect phase. However, it shows the significant magnitude error in the high-frequency region (Dyer & Dyer, 2000; Getu, 2020).

Case-II (when $\delta\phi \neq 0$ and $\delta\omega \rightarrow 0$)

This incorporates the number of operators proposed by Gupta et al., Upadhyay, Apoorva et al., and others (Aggarwal et al., 2017; Al-Alaoui, 2007, 2011a; Goswami et al., 2020, 2021; Gupta et al., 2010; Ngo, 2006; Pei & Hsu, 2008; Schneider et al., 1994; Upadhyay, 2012;

Upadhyay & Singh, 2011). They provide minimum variation in matching the magnitude response yet do not yield the perfect phase as bilinear transform does. Due to this mismatch of the phase response, these operators cannot be considered as a perfect *s*-to-*z* plane transforms in the true sense.

Hence, it is observed that there should be a trade-off between the bilinear transform and other transforms, which confers the least magnitude and phase error with reference to the ideal. Therefore, the proposed design attempts to match the magnitude and phase response with the ideal and provides a minimum error, i.e., $\delta\omega \rightarrow 0$ and $\delta\phi \rightarrow 0$.

3. Extended bilinear transforms

The most preferably used first-order bilinear transform is derived from the expansion of $z = e^{sT}$ or equivalently $s = \ln(z)/T$ of the series given below (Dyer & Dyer, 2000).

$$\frac{ln(z)}{T} = \frac{2}{T}\left[\frac{z-1}{z+1} + \frac{1}{3}\left(\frac{z-1}{z+1}\right)^3 + \frac{1}{5}\left(\frac{z-1}{z+1}\right)^5 + ..\right] \tag{4}$$

where $ln(z)$ is the natural logarithm of z. Substituting $z = e^{j\omega}$ in Eq. (4) results

$$\frac{ln(e^{j\omega})}{T} = \frac{2}{T}\left[\frac{e^{j\omega}-1}{e^{j\omega}+1} + \frac{1}{3}\left(\frac{e^{j\omega}-1}{e^{j\omega}+1}\right)^3 + \frac{1}{5}\left(\frac{e^{j\omega}-1}{e^{j\omega}+1}\right)^5 + ..\right] \tag{5}$$

For $T = 1$, the corresponding frequency response can be written as

$$ln(e^{j\omega}) = \left[2j\tan\left(\frac{\omega}{2}\right) + j^3\frac{2}{3}\tan^3\left(\frac{\omega}{2}\right) + j^5\frac{2}{5}\tan^5\left(\frac{\omega}{2}\right) + ..\right]$$

$$= e^{j\pm\frac{\pi}{2}}\left[2\tan\left(\frac{\omega}{2}\right) - \frac{2}{3}\tan^3\left(\frac{\omega}{2}\right) + \frac{2}{5}\tan^5\left(\frac{\omega}{2}\right) + \ldots.\right] \tag{6}$$

where the magnitude is given as

$$\left|ln(e^{j\omega})\right| = \left|\left[2\tan\left(\frac{\omega}{2}\right) - \frac{2}{3}\tan^3\left(\frac{\omega}{2}\right) + \frac{2}{5}\tan^5\left(\frac{\omega}{2}\right) + \ldots.\right]\right|$$

It is used to approximate the magnitude response of the ideal Laplace operator (s). The truncation of Eq. (4) after the first-term leads to the first-order bilinear transform, but it does not follow the Laplace operator's magnitude response for the full Nyquist band. Therefore, to extend this approximation of the matching magnitude, the second and third term from the right-hand side (RHS) of Eq. (4) is considered. It results in the third-order and fifth-order transfer functions, respectively.

The magnitude response of bilinear transform and extended bilinear transform are shown in Figure 1. It describes that the first-order bilinear transform matches the ideal magnitude response up to 0.28π of the normalised Nyquist interval. Whereas the third-order and fifth-order bilinear transforms extend the matching magnitude response up to 0.4π and 0.48π, respectively, of the normalised Nyquist range.

The phase responses shown in Figure 2 demonstrate that the first-order bilinear transform's phase perfectly matches the ideal. The extended third and fifth-order bilinear transforms display the ideal correlation up to 0.666π and 0.952π, respectively, and shift to

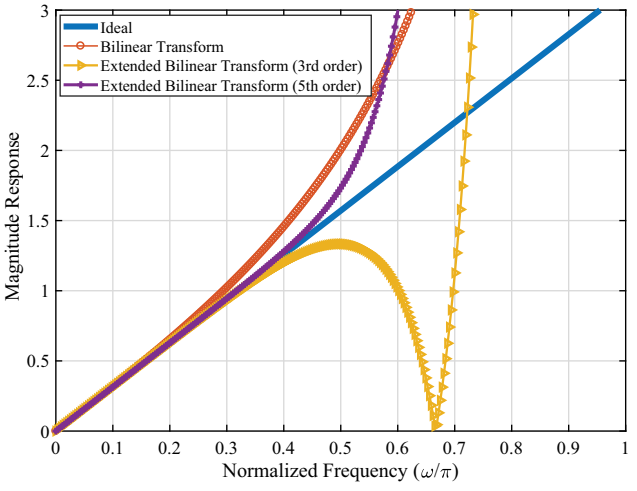

Figure 1. Magnitude response of the ideal, bilinear transforms, third-order bilinear transform, and fifth-order bilinear transform.

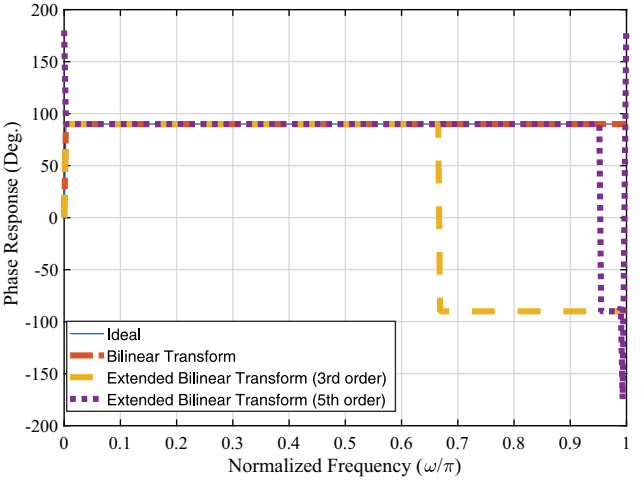

Figure 2. Phase response of the ideal, bilinear transforms, third-order bilinear transform, and fifth-order bilinear transform.

$-\pi/2$ after that. It is because the phase response associated with the magnitude response is a discontinuous linear function. Therefore, the phase will change from $+\pi/2$ to $-\pi/2$ or vice-versa, whenever the amplitude of $\ln(e^{j\omega})$ changes its sign (Rawat, 2014).

4. Proposed *s*-to-*z* transform

Taking advantage of the ideal phase of the bilinear and the extended bilinear transforms, the coefficients of series stated in Eq. (4) can be optimised to attain the ideal magnitude response.

Let

$$F(z) = \frac{z-1}{z+1} \tag{7}$$

The third-order transfer function is given by

$$F_1(z) = a_1 F(z) + a_2 F^3(z) \tag{8}$$

where a_1 and a_2 are the variables. Substitution of Eq. (7) in (8) yields

$$F_1(z) = \frac{(a_1+a_2)z^3 + (a_1-3a_2)z^2 - (a_1-3a_2)z - (a_1+a_2)}{z^3+3z^2+3z+1} \tag{9}$$

A general third-order transfer function can be expressed as

$$H(z) = \frac{A_1(z)}{A_2(z)} = \frac{b_0 z^3 + b_1 z^2 + b_2 z + b_3}{a_0 z^3 + a_1 z^2 + a_2 z + a_3} \tag{10}$$

Comparison of Eqs. (9) and (10) yields

$$b_0 = -b_3 = (a_1 + a_2) \tag{11}$$

$$b_1 = -b_2 = (a_1 - 3a_2) \tag{12}$$

$$a_0 = a_3 = 1 \tag{13}$$

$$a_1 = a_2 = 3 \tag{14}$$

The numerator coefficients of Eqs (9) and (10) are antisymmetric, whereas the denominator coefficients are symmetric. Therefore, Eq. (10) can be written as

$$H(\omega) = \frac{|A_1(\omega)|e^{j\theta_1(\omega)}}{|A_2(\omega)|e^{j\theta_2(\omega)}} = |A(\omega)|e^{j\theta(\omega)} \tag{15}$$

where

$$|A(\omega)| = \frac{|A_1(\omega)|}{|A_2(\omega)|} \tag{16}$$

$$\theta(\omega) = [\theta_1(\omega) - \theta_2(\omega)] \tag{17}$$

From Eqs. (10), (11) and (12), the following can be deduced

$$A_1(z) = b_0 z^3 + b_1 z^2 - b_1 z - b_0\big|_{z=e^{j\omega}}$$

$$A_1(\omega) = j e^{-j\frac{3}{2}\omega}\left[2b_0 \sin\left(\frac{3}{2}\omega\right) + 2b_1 \sin\left(\frac{1}{2}\omega\right)\right] \tag{18}$$

$$= e^{j\frac{\pi}{2}} e^{-j\frac{3}{2}\omega} \left[2b_0 \sin\left(\frac{3}{2}\omega\right) + 2b_1 \sin\left(\frac{1}{2}\omega\right) \right] \tag{19}$$

$$= |A_1(\omega)| e^{j\theta_1(\omega)} \tag{20}$$

where

$$\theta_1(\omega) = -\frac{3}{2}\omega + \frac{\pi}{2} \tag{21}$$

Similarly, from Eqs. (10), (13) and (14), the following can be deduced

$$A_2(z) = a_0 z^3 + a_1 z^2 + a_1 z + a_0 \big|_{z=e^{j\omega}}$$

$$A_2(\omega) = e^{-j\frac{3}{2}\omega} \left[2a_0 \cos\left(\frac{3}{2}\omega\right) + 2a_1 \cos\left(\frac{1}{2}\omega\right) \right] \tag{22}$$

$$= |A_2(\omega)| e^{j\theta_2(\omega)} \tag{23}$$

where

$$\theta_2(\omega) = -\frac{3}{2}\omega \tag{24}$$

Substituting of the values of $\theta_1(\omega)$ and $\theta_2(\omega)$ in Eq. (17) yields

$$\theta(\omega) = \pi/2 \tag{25}$$

Therefore, it is concluded that the $F_1(z)$ (Eq. (9)) provides the phase response $\pi/2$, and it will become $-\pi/2$ whenever its amplitude would change its sign. Now, for the magnitude response linearity, the coefficients a_1 and a_2 of the third-order transfer function are optimised by genetic algorithm (GA) (Mitchell, 1996), to minimise the difference between the Eq. (2) and the Eq. (9). The error objective function can be represented by

$$E = |(|f(z)| - |F_1(z)|)||_{z=e^{j\omega}} \tag{26}$$

The optimum values of a_1 and a_2 are obtained as 1.965 and 0.427, respectively. Substitution of these values in Eq. (9) yields

$$F_1(z) = \frac{1}{T}\left(\frac{2.392z^3 + 0.684z^2 - 0.684z - 2.392}{z^3 + 3z^2 + 3z + 1}\right) \tag{27}$$

Hence, Eq. (27) represents the optimum extended bilinear transform-based proposed *s*-to -*z* transform.

5. Simulation analysis of the proposed transform and comparison with the extended bilinear transforms

Figure 3 portrays the comparison of the magnitude response of the bilinear transform, extended bilinear transform, and the proposed transform. It is evident from Figure 3 that the proposed transform ($F_1(z)$) provides linearity up to 0.5π and matches the ideal magnitude for a wide range compared to bilinear, and extended bilinear transforms.

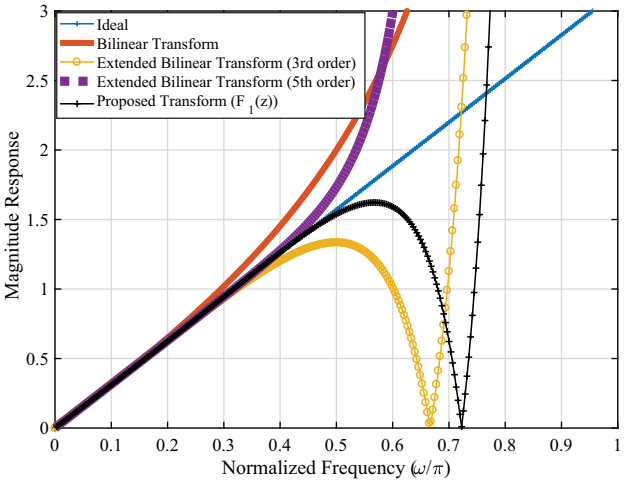

Figure 3. Comparison of the absolute magnitude errors of the bilinear transforms, third-order bilinear transform, fifth-order bilinear transform, and the proposed transform with ideal.

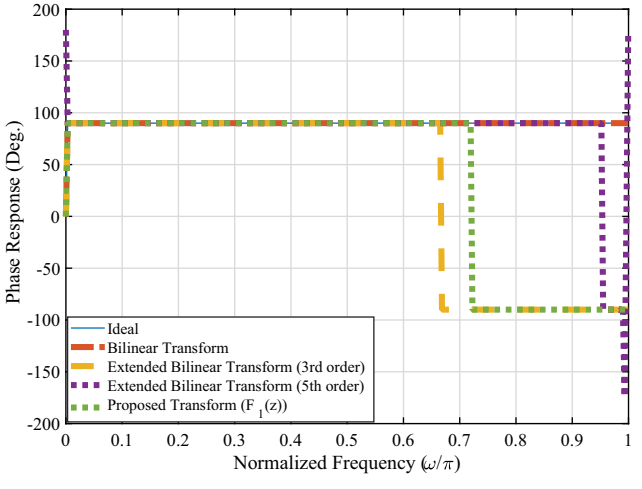

Figure 4. Phase responses of the ideal, bilinear transforms, third-order bilinear transform, fifth-order bilinear transform and the proposed transform.

The phase response shown in Figure 4 demonstrates that the proposed transform provides the ideal phase up to 0.7224π of the whole Nyquist interval. However, the proposed transform is not providing the magnitude matching and ideal phase up to the full Nyquist band. Therefore, the extension of the matching bandwidth is required to cover the entire Nyquist interval.

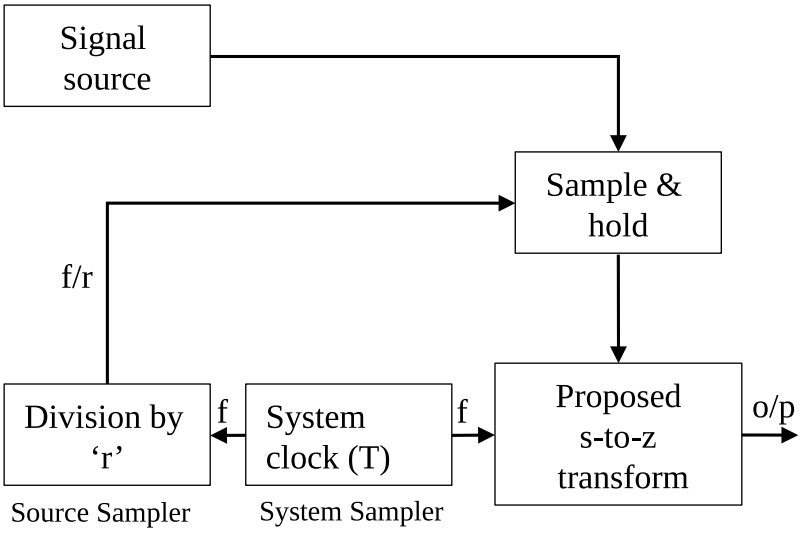

Figure 5. Implementation for the extension of the digital bandwidth.

6. Extension of bandwidth for the proposed transform

Figure 5 shows the multirate technique's implementation to extend the matching bandwidth $0 \leq \omega \leq 0.5\pi$ of the proposed transform. A high-frequency system clock shown in Figure 5 gets split into two. One clock provides the system delay $(z')^{-1}$, where $z'=(z)^{1/r}$, and the other clock is used by source sampler to sample the signal after getting divided by the factor r (Laakso et al., 1996). The sampled signal acquired by low sampling frequency is then interpolated and resampled by a high-frequency system clock. It provides stretching of the matching magnitude region $0 \leq \omega \leq 0.5\pi$ up to the complete Nyquist interval. Here, r should be chosen as binary power such that the splitting of the clock can be done using a binary divider chain (Devate et al., 2014, 2015). Hence, the least possible value of dividing factor r has been considered to avoid the clock synchronisation problem. Therefore, Eq. (10) can be written as

$$H(z') = r\frac{b_0 z'^3 + b_1 z'^2 + b_2 z' + b_3}{a_0 z'^3 + a_1 z'^2 + a_2 z' + a_3} \tag{28}$$

For $r = 2$, Eq. (28) can be written as

$$F_1(z') = 2\frac{2.392z'^3 + 0.684z'^2 - 0.684z' - 2.392}{z'^3 + 3z'^2 + 3z' + 1} \tag{29}$$

which is the transfer function of the proposed transform after utilising the concept of multirate technique.

7. Comparison with the Existing s-to-z Transforms

In 2011, Al-Alaoui proposed the design of a three-segment third-order differentiator, which was derived from the integration rules and optimisation (Al-Alaoui, 2011a). In another design, Nam Ngo applied the newton-cotes integration method to design a third-order differentiator (Ngo, 2006). Gupta et al. suggested the third-order design of a wideband differentiator by employing the linear programming (LP) technique in 2010 (Gupta et al., 2010). Moreover, in 2017, Apoorva et al. proposed a third-order differentiator by using a L_1 bat algorithm-based differentiator (Aggarwal et al., 2017). The transfer functions of all the operators mentioned above are enlisted in Table 1.

Figures 6 and 7, respectively, compare the magnitude and phase responses of the ideal, proposed transform, and the transforms enlisted in Table 1. Figure 8 shows the absolute magnitude error comparison of all the mentioned transforms with the ideal. Table 2 enlists the statistical analysis in terms of MAME (dB) and MAPE (dB). The proposed transform manifests a much linear magnitude response as compared to the other mentioned transforms. The proposed transform's absolute magnitude error remains less than 0.018 for $0 \leq \omega \leq 0.92\pi$ and 0.065 for the full band. The phase response of the proposed transform perfectly matches the ideal response for the entire Nyquist interval. The statistical conclusion made from Table 2 states that the proposed transform outperforms the other transform proposed by Al-Alaoui, Nam Quo, and Gupta et al. Though it remains

Table 1. Transfer functions of existing *s*-to-*z* transforms.

Transformation	Mapping Function/Transform
Al-Alaoui three-segment (Al-Alaoui, 2011a)	$\frac{1}{T}\left(\frac{0.0190z^3-0.0290z^2+1.1230z-1.1810}{z^3+0.1846z^2-0.0017z+0.0348}\right)$
Nam Quoc Ngo (Ngo, 2006)	$\frac{1}{T}\left(\frac{2.7925z^2(z-1)}{(2.3658)(z+(1/2.3658))(z^2-0.2605z+0.047}\right)$
Gupta et al. (Gupta et al., 2010)	$\frac{1}{T}\left(\frac{z^2(z-1)}{0.329z^3+0.8677z^2-0.1694z+0.0038}\right)$
Apoorva et al. (Aggarwal et al., 2017)	$\frac{1}{T}\left(\frac{0.2232z^3+0.5343z^2-0.2803z-0.4773}{0.4942z^3+0.6953z^20.2550z+0.0173}\right)$

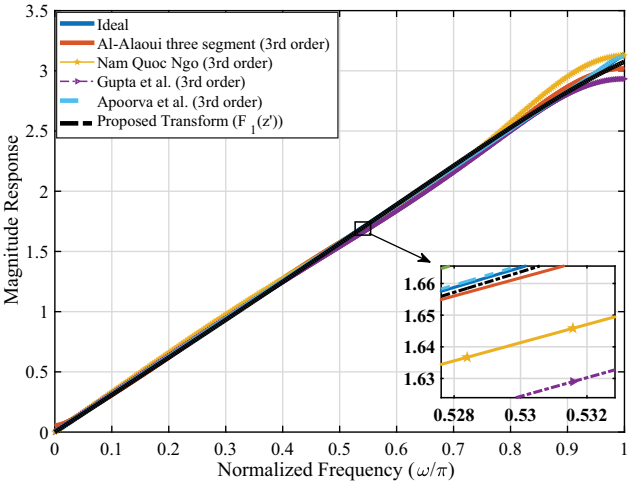

Figure 6. Magnitude responses of the ideal, the proposed transform, and the existing transforms.

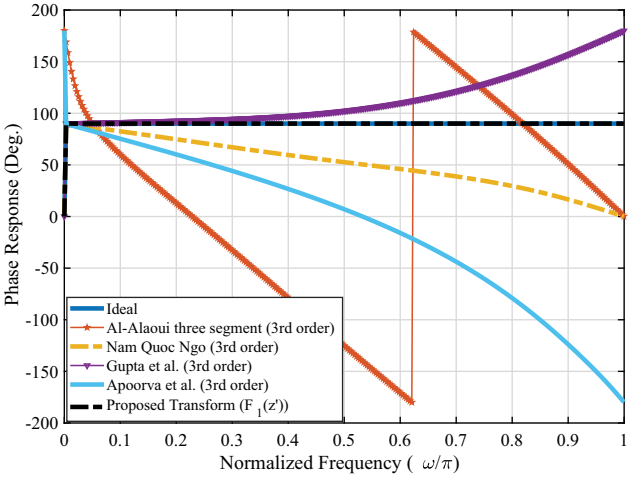

Figure 7. Phase responses of the ideal, the proposed transform, and the existing transforms.

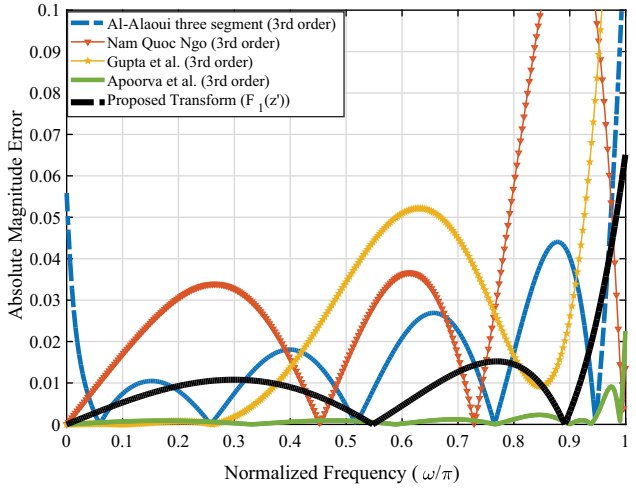

Figure 8. Comparison of the absolute magnitude errors of the proposed transform and existing transforms with the ideal.

Table 2. Comparison of errors of the existing transforms with the proposed transform.

Transformation	MAME, (dB)	MAPE, (dB)
Al-Alaoui three-segment rule,(3rd order) (Al-Alaoui, 2011a)	−35.0897	4.7075
Nam Quoc Ngo's (3rd order) (Ngo, 2006)	−28.898	−3.4139
Gupta et al. (3rd order) (Gupta et al., 2010)	−31.4049	−7.70
Apoorva et. al. (3rd order) (Aggarwal et al., 2017)	−59.1721	4.80
Proposed Transform ($F_1(z')$)	−40	−132.04

comparable with the design proposed by Apoorva et al. in terms of MAME. However, in terms of MAPE, the proposed transform performs best compared to the other transforms enlisted in Table 1. Therefore, the proposed transform manifests a suitable trade-off between matching the ideal magnitude and the phase response. Consequently, it is tactical to utilise the proposed operator for analog to digital domain transformation in the filter designing.

8. Example

To validate the proposed *s*-to-*z* operator, an example of an IIR Butterworth low-pass filter with second-order is taken into consideration. The analog transfer function is stated below as (Mishra et al., 2019)

$$H_1(s) = \frac{0.5631}{s^2 + 1.061s + 0.5631}$$

The enlisted *s*-to-*z* operators in Table 5.1 and the proposed transform $F_1(z')$ have been applied to the analog transfer function $H_1(s)$. The result in magnitude and phase responses have been portrayed in Figures 9 and 10, respectively. The responses depict that the proposed transform provides a better correlation with the corresponding analog response than others. The AME response, shown in Figure 11, shows that the proposed transform provides the least magnitude error. The maximum magnitude error produced is restricted up to 0.015, which confirms the proposed transform's efficacy.

9. Conclusion

In this paper, a new design of the *s*-to-*z* transform has been presented. It has been derived by optimising the coefficients of the logarithmic series followed by extending its matching bandwidth up to full Nyquist interval. The proposed *s*-to-*z* operator provides MAME

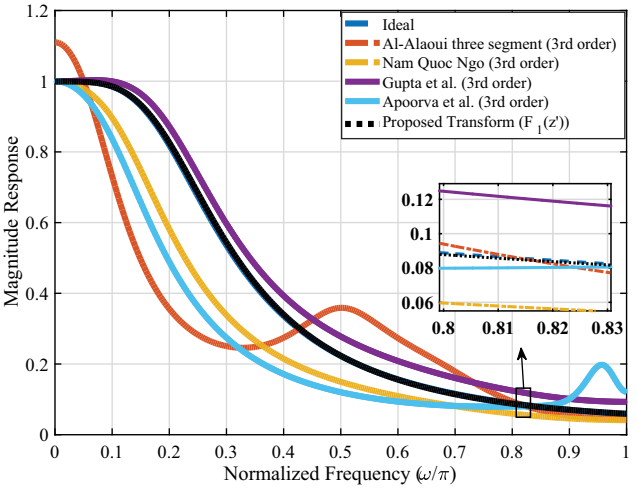

Figure 9. Comparison of the magnitude responses of the low-pass filter.

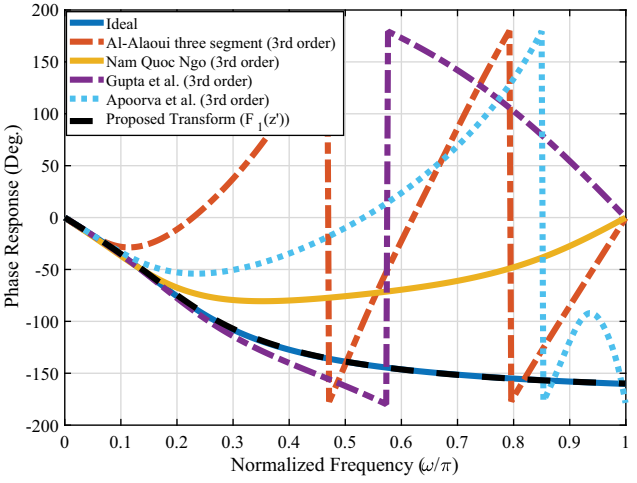

Figure 10. Comparison of the phase responses of the low-pass filter.

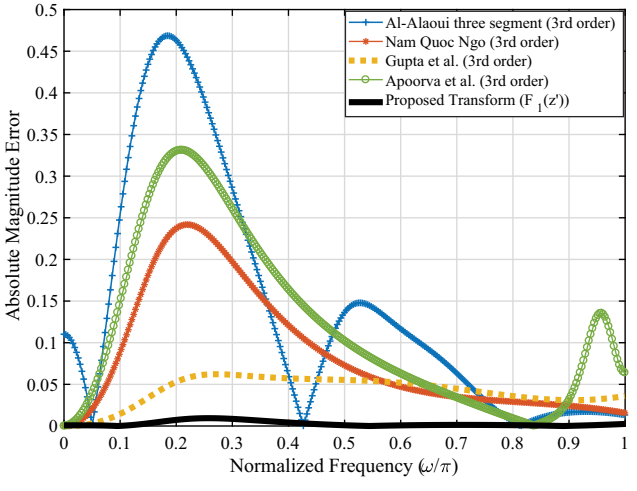

Figure 11. Comparison of the absolute magnitude errors of the low-pass filter.

and MAPE as -40 dB and -132.04 dB, respectively, and performs better than all the existing *s*-to-*z* operators. The proposed transform has also been applied in transforming a filter from the analog domain to the digital domain. It provides the accurate frequency responses than the existing transforms, which validates its applicability. Therefore, the proposed *s*-to-*z* transform can be employed as an alternative to the existing analog-to-digital transforms in digital filter designing.

Disclosure statement

No potential conflict of interest was reported by the author(s).

References

Aggarwal, A., Rawat, T. K., & Upadhyay, D. K. (2015). Optimal design of FIR high pass filter based on L_1 error approximation using a real coded genetic algorithm. *Engineering Science and Technology, an International Journal*, *18*(4), 594–602. https://doi.org/10.1016/j.jestch.2015.04.004

Aggarwal, A., Rawat, T. K., & Upadhyay, D. K. (2017). Optimal design of L_1-norm based IIR digital differentiators and integrators using the bat algorithm. *IET Signal Processing*, *11*(1), 26–35. https://doi.org/10.1049/iet-spr.2016.0010

Al-Alaoui, M. A. (2007). Novel approach to analog-to-digital transforms. *IEEE Transactions on Circuits and Systems I: Regular Papers*, *54*(2), 338–350. https://doi.org/10.1109/TCSI.2006.885982

Al-Alaoui, M. A. (2011a). Novel FIR approximations of IIR differentiators with applications to image edge detection. *18th IEEE International Conference on Electronics, Circuits, and Systems* (pp. 554–558). Lebanon.

Al-Alaoui, M. A., & Baydoun, M. (2013). Novel wide band digital differentiators and integrators using different optimization techniques. *International Symposium on Signals, Circuits and Systems (ISSCS2013). IEEE* (pp. 1–4).Iasi, Romania.

Deng, T. B. (2016). Design of recursive variable digital filters with theoretically guaranteed stability. *International Journal of Electronics*, *103*(12), 2013–2028. https://doi.org/10.1080/00207217.2016.1175033

Devate, J., Kulkarni, S. Y., & Pai, K. R. (2014). Wideband IIR digital integrator and differentiator. *Proceedings of International Conference on Circuits, Communication, Control and Computing* . IEEE. (pp. 81–84).Chennai, India.

Devate, J., Kulkarni, S. Y., & Pai, K. R. (2015). Wideband differentiator and integrator with ideal phase response. *Canadian Journal of Electrical and Computer Engineering*, *38*(4), 294–299. https://doi.org/10.1109/CJECE.2015.2444443

Dyer, S. A., & Dyer, J. S. (2000). The bilinear transformation. *IEEE Instrumentation & Measurement Magazine*, *3*(1), 30–34. https://doi.org/10.1109/5289.823821

Getu, B. N. (2020). Digital IIR Filter Design using Bilinear Transformation in MATLAB. *International Conference on Communications, Computing, Cybersecurity, and Informatics (CCCI)* (pp. 1–6). https://doi.org/10.1109/CCCI49893.2020.9256625 .Sharjah,United Arab Emirates.

Goswami, O. P., Rawat, T. K., & Upadhyay, D. K. (2020). A novel approach for the design of optimum IIR differentiators using fractional interpolation. *Circuits Systems and Signal Processing*, *39*(3), 1688–1698. https://doi.org/10.1007/s00034-019-01211-0

Goswami, O. P., Rawat, T. K., & Upadhyay, D. K. (2021). Fractional Interpolation and Multirate Technique Based Design of Optimum IIR Integrators and Differentiators. *International Journal of Electronics*, 1–15. https://doi.org/10.1080/00207217.2020.1870730

Gupta, M., Jain, M., & Kumar, B. (2010). Novel class of stable wideband recursive digital integrators and differentiators. *IET Signal Processing*, *4*(5), 560–566. https://doi.org/10.1049/iet-spr.2009.0030

Gupta, M., Relan, B., Yadav, R., & Aggarwal, V. (2014). Wideband digital integrators and differentiators designed using particle swarm optimization. *IET Signal Processing*, *8*(6), 668–679. https://doi.org/10.1049/iet-spr.2013.0011

Kim, T. I., Han, J. S., Oh, T. H., Kim, Y. S., Lee, S. H., & Cho, D. I. (2019). A new accurate discretization method for high-frequency component mechatronics systems. *Mechatronics*, *62*, 102250. https://doi.org/10.1016/j.mechatronics.2019.102250

Laakso, T. I., Valimaki, V., Karjalainen, M., & Laine, U. K. (1996). Splitting the unit delay: Tools for fractional delay filter design. *IEEE Signal Processing Magzine*, *13*(1), 30–60. https://doi.org/10.1109/79.482137

Mishra, S. K., Upadhyay, D. K., & Gupta, M. (2019). Search of Optimal s-to-z Mapping Function for IIR Filter Designing without Frequency Pre-warping. *IETE Journal of Research*, 1–9. https://doi.org/10.1080/03772063.2019.1569484

Mitchell, M. (1996). *An Introduction to Genetic Algorithms*. MIT Press Cambridge.

Ngo, N. Q. (2006). A new approach for the design of wideband digital integrator and differentiator. *IEEE Transaction on Circuits and Systems II: Express Briefs*, *53*(9), 936–940. https://doi.org/10.1109/TCSII.2006.881806

Pei, S. C., & Hsu, H. J. (2008). Fractional bilinear transform for analog-to-digital conversion. *IEEE Transaction on Signal Processing*, *56*(5), 2122–2127. https://doi.org/10.1109/TSP.2007.912250

Rawat, T. K. (2014). *Digital Signal Processing*. Oxford University Press.

Schneider, A. M., Anuskiewicz, J. A., & Barghouti, I. S. (1994). Accuracy and stability of discrete-time filters generated by higher-order s-to-z mapping functions. *IEEE Transactions on Automatic Control*, *39*(2), 435–441. https://doi.org/10.1109/9.272353

Stosovic, M. A., Topisirovic, D., & Litovski, V. (2019). Frequency and time domain comparison of selective polynomial filters with corrected phase characteristics. *International Journal of Electronics*, *106*(5), 770–784. https://doi.org/10.1080/00207217.2019.1570560

Tsai, J. T., & Chou, J. H. (2006). Design of optimal digital IIR filters by using an improved immune algorithm. *IEEE Transaction on Signal Processing*, *54*(12), 4582–4596. https://doi.org/10.1109/TSP.2006.881248

Upadhyay, D. K. (2012). Class of recursive wideband digital differentiators and integrators. *Radioengineering*, *21*(3), 904–910. https://www.radioeng.cz/fulltexts/2012/12_03_0904_0910.pdf

Upadhyay, D. K., & Singh, R. K. (2011). Recursive wideband digital differentiator and integrator. *Electronics Letters*, *47*(11), 647–648. https://doi.org/10.1049/el.2011.0420

Xu, Y., Dai, T., Sycara, K. P., & Lewis, M. (2010). Service level differentiation in multi-robots control. *IEEE/RSJ International Conference on Intelligent Robots and Systems* (pp. 2224–2230).Taipei, Taiwan.